Supporting Information

Super absorbent conjugated microporous polymers: a synergistic structural effect on exceptional uptake of amines

Xiaoming Liu, Yanhong Xu, Zhaoqi Guo, Atsushi Nagai, and Donglin Jiang*
Department of Materials Molecular Science, Institute for Molecular Science, National Institute of Natural Sciences, 5-1 Higashiyama, Myodaiji, Okazaki 444-8787, Japan

Section 1. Materials and Methods

Organic solvents for reaction were distilled over appropriate drying reagents under argon or obtained as dehydrated reagents from Kanto Chemicals. Deuterated solvents for NMR measurement were obtained from Cambridge Isotope Laboratories, Inc. *p*-Bromobenzaldehyde, pyrrole, acetic acid, and Ni(COD)$_2$ were obtained from Aldrich. 2,2'-bipyridine, COD, zinc acetate hydrate, copper acetate hydrate, and cobalt acetate tetrahydrate were obtained from Kanto Chemicals.

Synthesis of 5, 10, 15, 20-tetrakis(4'-bromophenyl)porphyrin

A mixture of *p*-bromobenzaldehyde (3.72 g, 20 mmol) in nitrobenzene (100 mL) and acetic acid (150 mL) was heated up to 120 °C and was added with freshly distilled pyrrole (1.4 mL, 20 mmol). The mixture was stirred at 120 °C for 1h and cooled to room temperature. The dark violet precipitate was collected by filtration and washed with methanol (50 mL × 3). The product was purified by recrystallization twice from CHCl$_3$/MeOH, to give 5,10,15, 20-tetrakis(4'-bromophenyl)porphyrin as violet crystal (1.38 g) in 30% yield. ^{1}H NMR (CDCl$_3$, 400 MHz): δ (ppm) –2.87 (s, 2H, N–H), 7.91 (d, 8H, J = 8.2 Hz, Ar–H), 8.07 (d, 8H, J = 8.2 Hz, Ar–H), and 8.84 (s, 8H, pyrrole–H). MALDI-TOF MS: *m*/*z* 929.89, calcd. for $C_{44}H_{26}Br_4N_4$; found, $[M + H]^+$ 929.47.

Synthesis of zinc (II) 5,10,15,20-tetrakis-(4'-bromophenyl)porphyrin (ZnP$_1$)

To a mixture of 5,10,15,20-tetrakis-(4'-bromophenyl)porphyrin (360 mg, 0.39 mmol), CHCl$_3$ (20 mL) and AcOH (20 mL) was added with Zn(OAc)$_2$•2H$_2$O (848 mg, 3.86 mmol). After stirred at 120 °C for 1.5 h, the precipitate was filtered and washed with MeOH (10 mL × 3). The product was isolated by column chromatography as a purple solid (348 mg, 90% yield). ^{1}H

NMR ($CDCl_3$, 400 MHz): δ (ppm) 7.90 (d, 8H, $J = 8.33$ Hz, Ar–H), 8.07 (d, 8H, $J = 8.33$ Hz, Ar–H), 8.94 (s, 8H, pyrrole–H). MALDI-TOF MS: m/z 993.80, calcd. for $C_{44}H_{24}Br_4N_4Zn$; found, $[M]^+$ 992.71. IR (KBr, ν; cm^{-1}): 1519, 1471, 1390, 1334, 1205, 1175, 1070, 1002, 797, 1070, 721, and 465. UV-Vis (λ; nm): 430, 592, and 624.

Synthesis of copper (II) 5,10,15,20-tetrakis-(4'-bromophenyl)porphyrin (CuP_1)

To a mixture of 5,10,15,20-tetrakis-(4'-bromophenyl)porphyrin (180 mg, 0.19 mmol), $CHCl_3$ (12 mL), and AcOH (12 mL) was added with $Cu(OAc)_2$•H_2O (385 mg, 1.93 mmol). After stirred at 120 °C for 1.5 h, the precipitate was filtered and washed with MeOH (10 mL × 3). The product was isolated by column chromatography as a red solid (159 mg, 85% yield). MALDI-TOF MS: m/z 990.80, calcd for $C_{44}H_{24}Br_4N_4Cu$; found, $[M]^+$ 990.38. IR (KBr, ν; cm^{-1}): 1585, 1534, 1479, 1441, 1386, 1340, 1305, 1239, 1206, 1070, 1003, 796, 718 and 478. UV-Vis (λ; nm): 427, 545, and 587.

Synthesis of cobalt (II) 5,10,15,20-tetrakis-(4'-bromophenyl)porphyrin (CoP_1)

To a mixture of 5,10,15,20-tetrakis-(4'-bromophenyl)porphyrin (232 mg, 0.25 mmol), $CHCl_3$ (12 mL), and AcOH (12 mL) was added with $Co(OAc)_2$•$4H_2O$ (622 mg, 2.50 mmol). After stirred at 120 °C for 1.5 h, the precipitate was filtered and washed with MeOH (10 mL × 3). The product was isolated by column chromatography as a brown solid (202 mg, 82% yield). MALDI-TOF MS: m/z 986.80, calcd. for $C_{44}H_{24}Br_4N_4Co$; found, $[M]^+$ 986.39. IR (KBr, ν; cm^{-1}): 1584, 1537, 1481, 1443, 1387, 1340, 1237, 1199, 1068, 1002, 880, 796, 711, and 482. UV-Vis (λ; nm): 442, 536, 624, and 661.

Synthesis of ZnP_1-CMP

1,5-Cyclooctadiene (62 mg, 0.57 mmol) was added to a DMF solution (8 mL) of bis(1,5-cyclooctadiene)nickel(0) (159 mg, 0.57 mmol) and 2,2'-bipyridyl (90 mg, 0.57 mmol) and the mixture was heated at 80 °C for 1 h. To the mixture was added with ZnP_1 (120 mg, 0.12 mmol) and the mixture was stirred at 80 °C for 72 h to give a deep purple suspension. After cooling to room temperature, the mixture was added with acetate acid (10 mL) and stirred at room temperature for 10 h. After filtration, the residue was washed with $CHCl_3$ (30 mL × 5), THF (30 mL × 5), and water (30 mL × 5), respectively, and dried in vacuum, to give ZnP_1-CMP as a deep-red powder (100 mg, 98% yield). Elemental analysis (wt%) calcd. For $\{C_{44}H_{24}N_4Zn\}_n$: C 78.40, H 3.59, N 8.31; found: C 75.53, H 4.05, N 7.41. IR (KBr, ν; cm^{-1}): 3025, 1601, 1491, 1345, 1206, 1072, 1002 ($\delta_{Zn–N}$), 799, 718, and 566. UV-Vis (λ; nm): 462, 558, 602, and 658.

Synthesis of CuP_1-CMP

1,5-Cyclooctadiene (62 mg, 0.57 mmol) was added to a DMF solution (8 mL) of bis(1,5-cyclooctadiene)nickel(0) (159 mg, 0.57 mmol) and 2,2'-bipyridyl (90 mg, 0.57 mmol) and the mixture was heated at 80 °C for 1 h. To the mixture was added with CuP_1 (120 mg, 0.12 mmol) and the mixture was stirred at 80 °C for 72 h to give a deep purple suspension. After cooling to room temperature, the mixture was added with acetate acid (10 mL) and stirred at room temperature for 10 h. After filtration, the residue was washed with $CHCl_3$ (30 mL × 5), THF (30 mL × 5), and water (30 mL × 5), respectively, and dried in vacuum, to give CuP_1-CMP as a deep-red powder (77 mg, 94% yield). Elemental analysis (wt%) calcd. For $\{C_{44}H_{24}N_4Cu\}_n$: C 78.61, H 3.60, N 8.33; found: C 72.72, H 3.47, N 7.66. IR (KBr, ν; cm^{-1}): 3024, 1600, 1491, 1342, 1201, 1080, 1003 (δ_{Cu-N}), 801, 718, and 559. UV-Vis (λ; nm): 454, 548, and 595.

Synthesis of CoP_1-CMP

1,5-Cyclooctadiene (63 mg, 0.58 mmol) was added to a DMF solution (8 mL) of bis(1,5-cyclooctadiene)nickel(0) (161 mg, 0.58 mmol) and 2,2'-bipyridyl (91 mg, 0.58 mmol) and the mixture was heated at 80 °C for 1 h. To the mixture was added with CoP_1 (120 mg, 0.12 mmol) and the mixture was stirred at 80 °C for 72 h to give a deep purple suspension. After cooling to room temperature, the mixture was added with acetate acid (10 mL) and stirred at room temperature for 10 h. After filtration, the residue was washed with $CHCl_3$ (30 mL × 5), THF (30 mL × 5), and water (30 mL × 5), respectively, and dried in vacuum, to give CoP_1-CMP as a brown powder (78 mg, 96% yield). Elemental analysis (wt%) calcd. For $\{C_{44}H_{24}N_4Co\}_n$: C 79.16, H 3.62, N 8.39; found: C 72.12, H 4.52, N 6.45. IR (KBr, ν; cm^{-1}): 3025, 1701, 1608, 1545, 1493, 1348, 1262, 1071, 1003 (δ_{Co-N}), 805, 715, and 566. UV-Vis (λ; nm): 466, 543, and 624.

Synthesis of ZnP_2-CMP

A mixture of ZnP_1 (90 mg, 0.09 mmol) and biphenyl-4,4'-diboronic acid (43.5 mg, 0.18 mmol) in dioxane (8 mL) was degassed by three freeze–pump–thaw cycles. To the mixture was added an aqueous solution (2.0 mL) of K_2CO_3 (66.36 mg, 0.48 mmol) and tetrakis(triphenylphosphine)palladium(0) (10.2 mg, 9 μmol). The mixture was degassed by three freeze–pump–thaw cycles, purged with Ar, and stirred at 100 °C for 48 h. The mixture was allowed to cool at room temperature and poured into water. The precipitate was collected by filtration, washed with water, THF, methanol, and acetone, and rigorously washed by Soxhlet extractions for 24 h with THF, methanol, and acetone as solvent, respectively, and dried in vacuum to give ZnP_2-CMP (83.05 mg) as a dark green solid in 94 % yield. Elemental analysis (%) calcd. for $\{C_{68}H_{40}ZnN_4\}_n$ (theoretical formula for an infinite 2D polymer): C 83.47, H 4.12, N 5.73; found: C 75.49, H 4.47, N 5.37. IR (KBr, ν; cm^{-1}): 3024, 1602, 1493, 1345, 1206, 1071, 1001, 798, 717, and 566. UV-Vis (λ; nm): 452, 566, and 608.

Synthesis of ZnP$_1$-LP

A mixture of ZnP$_1$ (50 mg, 0.075 mmol) and 1,4-phenyldiboronic acid (12.45 mg, 0.075 mmol) in dioxane (4 mL) was degassed by three freeze–pump–thaw cycles. To the mixture was added an aqueous solution (3.0 mL) of K_2CO_3 (82.80 mg, 0.60 mmol) and tetrakis(triphenylphosphine)palladium(0) (8.67 mg, 7.5 μmol). The mixture was degassed by three freeze–pump–thaw cycles, purged with Ar, and stirred at 100 °C for 48 h. The mixture was allowed to cool at room temperature and poured into water. The precipitate was collected by filtration, washed with water, THF, methanol, and acetone, rigorously washed by Soxhlet extractions for 24 h with THF, methanol, and acetone as solvent, respectively, and dried in vacuum to give ZnP$_1$-LP (32.13 mg) as a dark green solid in 73% yield. Elemental analysis (%) calcd. for $\{C_{38}H_{22}ZnN_4\}_n$ (Theoretical formula for an infinite linear polymer): C 76.07, H 3.70, N 9.34; found: C 68.43, H 3.16, N 7.31. IR (KBr, ν; cm^{-1}): 1600, 1521, 1390, 1294, 1060, 996, 783, 699, and 537.

^{1}H spectra were recorded on a JEOL model JNM-LA400 NMR spectrometer, where chemical shifts (δ in ppm) were determined with a residual proton of the solvent as standard. Matrix-assisted laser desorption ionization time-of-flight mass (MALDI-TOF MS) spectra were performed on an Applied Biosystems BioSpectrometry model Voyager-DE-STR spectrometer in reflector or linear mode using 9-nitroanthracene or dithranol as a matrix. Solid-state ^{13}C CP/MAS NMR measurements were performed on a JEOL model 920 MHz NMR spectrometer at a MAS rate of 15 kHz and a CP contact time of 2 ms. The diffuse reflectance spectra (Kubleka-Munk spectrum) were recorded on a JASCO model V-670 spectrometer equipped with integration sphere model IJN-727. Infrared spectra were recorded on a JASCO model FT IR-6100 Fourier transform infrared spectrophotometer. Elemental analyses were carried out on an Elementar model varioEL analyzer. Field emission scanning electron microscopy was performed on a JEOL model JEM-6700 microscope operating at an accelerating voltage of 5.0 kV. High resolution transmission electron microscopy was performed on a JEOL model JEM-3200 microscope. The sample was prepared by drop-casting a supersonicated methanol suspension of CMPs onto a copper grid. TGA measurements were carried out on a Mettler Toledo model TGA/SDTIA 851^e by heating the sample from 25 °C at a heating rate of 10 °C min^{-1}. Powder X-ray diffraction data were recorded on a Rigaku model RINT Ultima III diffractometer by depositing powder on glass substrate, from $2\theta = 1.5°$ to 60° with 0.02°

increment at 25 °C.

Nitrogen sorption isotherms were measured at 77 K with a Bel Japan Inc. model BELSORP-mini II analyzer. Before measurement, the samples were degassed in vacuum at 150 °C for more than 10 h. The Brunauer-Emmett-Teller (BET) method was utilized to calculate the specific surface areas and pore volume, the Saito-Foley method was applied for the estimation of pore size and pore size distribution.

The uptake of amine vapor was performed under ambient conditions (1 bar, 25 °C) in a vapor diffusion adsorption setup. The sample (10 mg) without any pretreatment to remove air in the pores was placed in a 10-mL vial, which was allowed to stand in a 50-mL vial containing 1-g amine. The 50-mL vial was then sealed with a cap and stood under ambient conditions for a week. The absorption levels off at one week for other amines tested, while aniline requires a longer time. The weight increment was investigated by TGA and was utilized for the evaluation of capacity. For each data, the experiments were carried out for 3 independent absorptions and the averaged value was utilized as the experimental capacity. The theoretical capacity was calculated by multiplying pore volume and amine density.

The uptake of amine liquid was performed under ambient conditions (1 bar, 25 °C) by the traditional method. A 20 mg CMP sample was ground with 2 mg PTFE (It does not show the absorption of amines!) to make a thin tape, which was dipped into the amine liquids for a designated period, the tape was then exposed to air for the evaporation of amine on surface. The increment in weight was utilized for the evaluation of absorption capacity. For each data, the absorption was carried out for 3 independent times and the averaged value was utilized as the final capacity.

The reusability of CMPs was tested under ambient conditions by repeating the uptake of pyridine vapor and TGA followed by vacuum evaporation. The sample was then cooled down in air at 25 °C for the next round cycle.

Section 2. FT IR Spectra

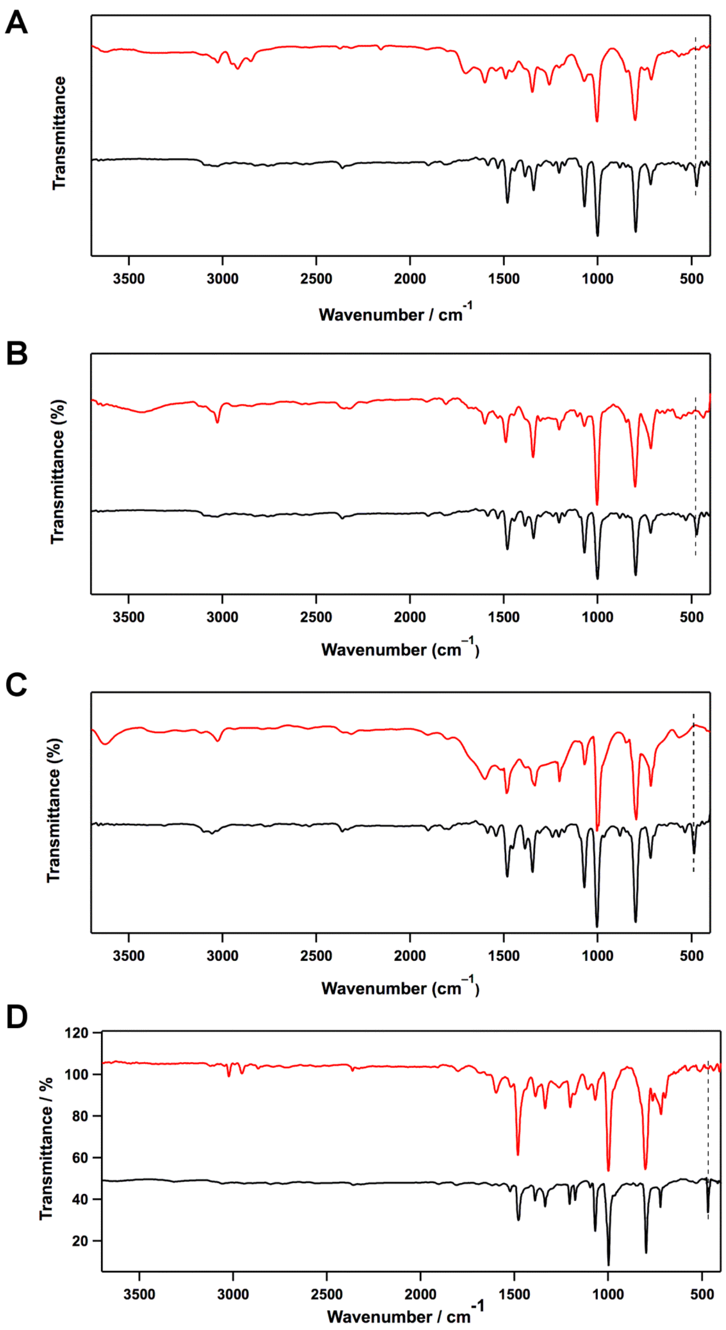

Figure S1. FT IR spectra of A) ZnP$_1$-CMP, B) CuP$_1$-CMP, C) CoP$_1$-CMP, and D) ZnP$_2$-CMP (black curves: MP$_1$; red curves: CMPs). The bands around 1000 cm^{-1} are the vibration bands due to the N–M bonds. The bands with dotted line are assigned to the C–Br bond.

Section 3. Solid State ^{13}C CP/MAS NMR Spectrum

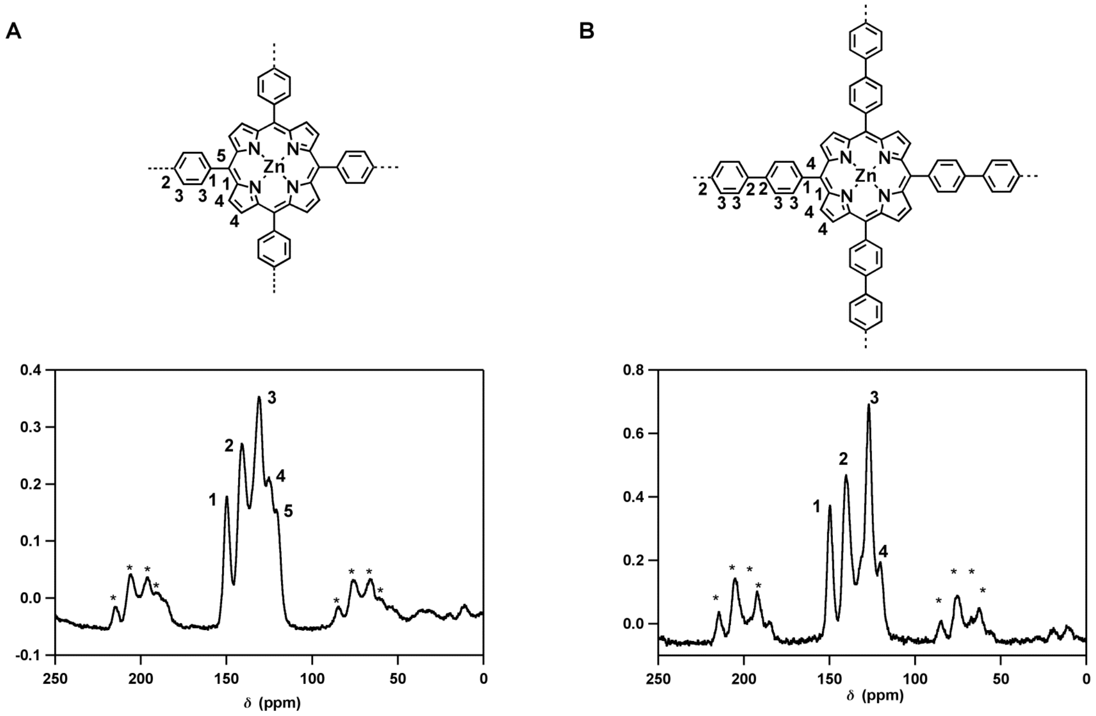

Figure S2. Solid-state ^{13}C CP/MAS NMR spectra of A) ZnP$_1$-CMP and B) ZnP$_2$-CMP, recorded at a CP contact time of 2 ms and a MAS rate of 15 kHz. Signals with * symbols are side peaks.

Section 4. UV-Vis Spectral Profiles

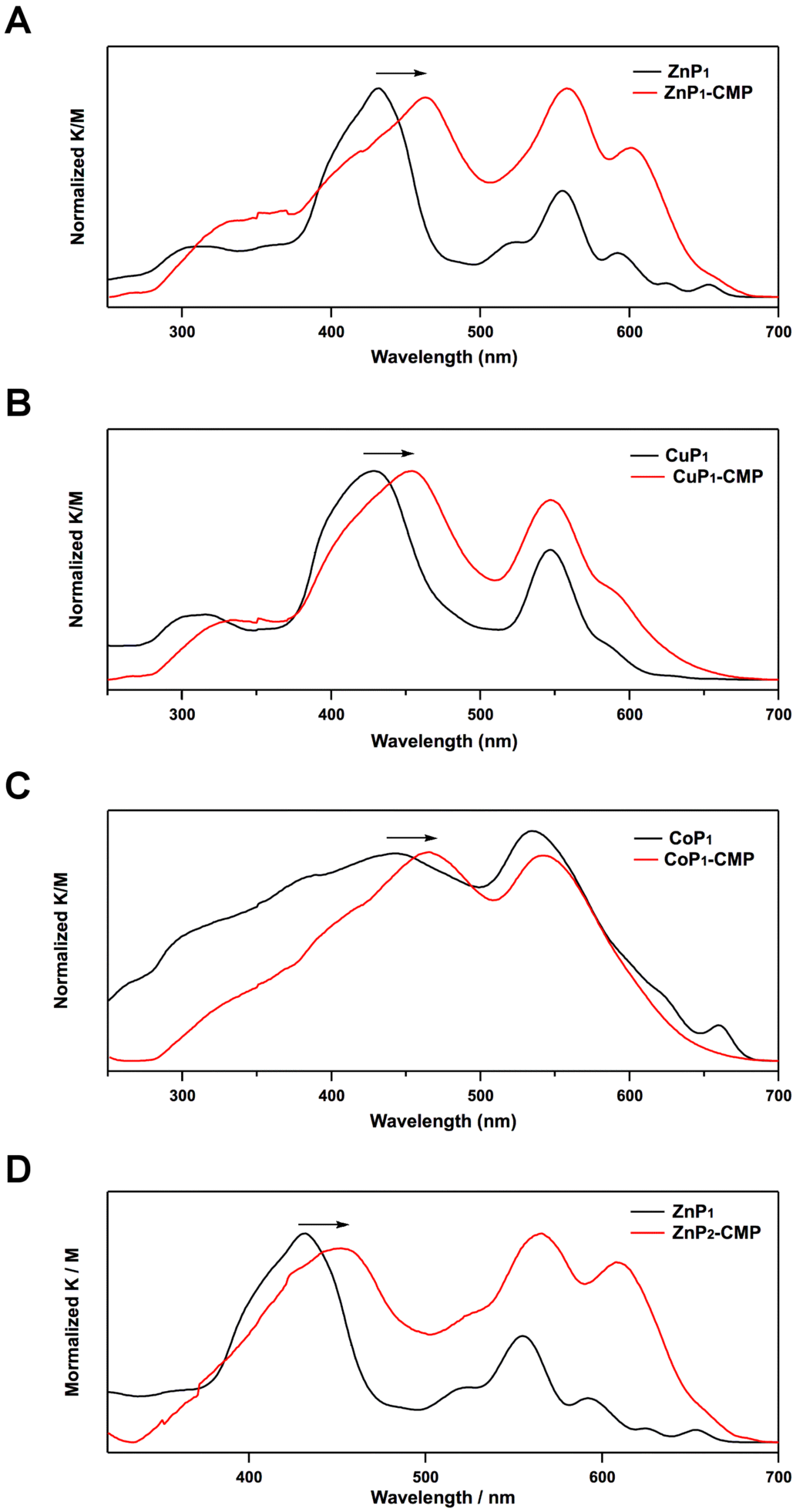

Figure S3. UV-Vis spectra of A) ZnP_1-CMP, B) CuP_1-CMP, C) CoP_1-CMP, and D) ZnP_2-CMP (red curves) and MP_1 (black curves).

Section 5. Powder X-Ray Diffraction

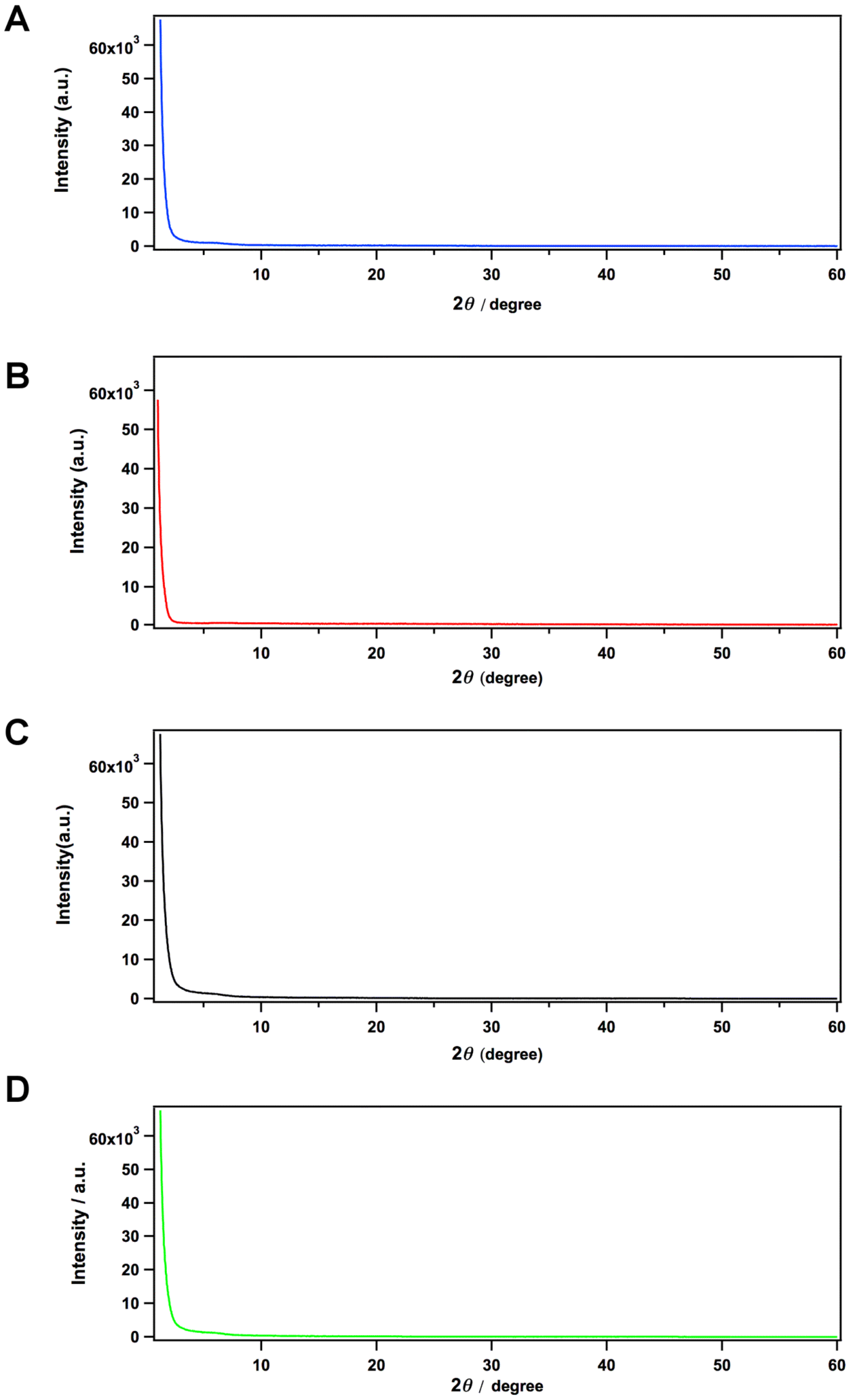

Figure S4. Powder X-ray diffraction patterns of A) ZnP_1-CMP, B) CuP_1-CMP, C) CoP_1-CMP, and D) ZnP_2-CMP.

Section 6. TGA Profiles

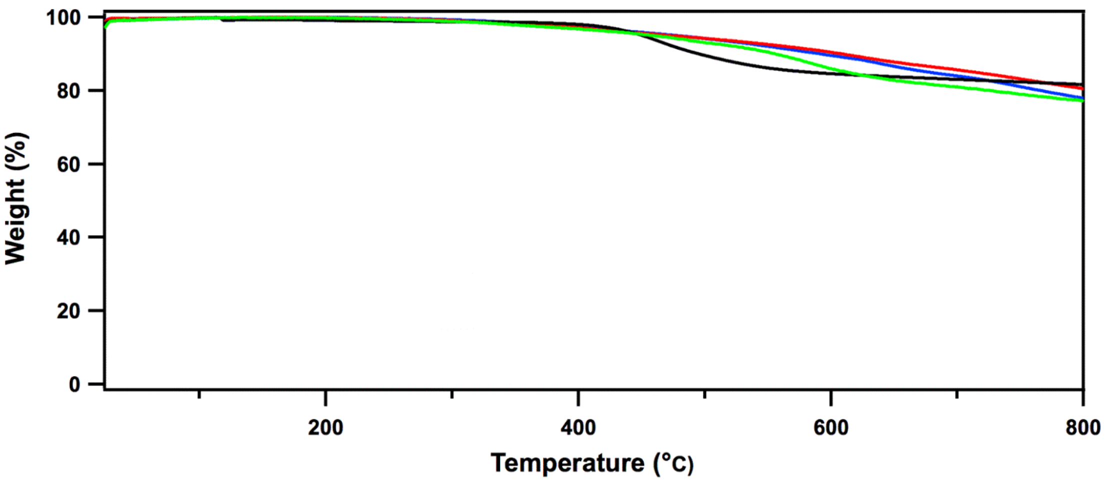

Figure S5. The TGA curves of ZnP$_1$-CMP (red), CuP$_1$-CMP (blue), CoP$_1$-CMP (green), and ZnP$_2$-CMP (black).

Section 7. Pore parameters and amine uptake capacity

Table 1. Pore parameters and amine uptake capacity of MP$_1$-CMPs, ZnP$_2$-CMP, ZnP$_1$-LP, and YP-17.

Porous Material	BET Surface area (m^2 g^{-1})	Pore Volume (cm^3 g^{-1})	Pore Size (nm)	Capacity (g$_{amine}$/g$_{CMP}$)						
				n-Propyl amine	*n*-Butyl amine	*n*-Hexyl amine	Diisobutyl amine	Dibutyl amine	Aniline	Pyridine
ZnP$_1$-CMP	1140	1.49	0.8-2	1.70[a]/5.1[b] (1.07)[c]	2.24/5.42 (1.10)	2.66/6.15 (1.14)	1.59/5.30 (1.14)	2.25/5.48 (1.13)	1.61/5.39 (2.22)	3.53/5.68 (1.46)
CuP$_1$-CMP	1247	1.49	0.8-2	2.40/3.30 (1.07)	2.52/3.88 (1.10)	3.81/5.40 (1.14)	1.87/4.85 (1.14)	1.95/5.18 (1.13)	1.24/5.59 (2.22)	3.58/5.42 (1.46)
CoP$_1$-CMP	1080	1.16	0.8-2	1.47/2.77 (0.83)	1.83/2.96 (0.86)	3.06//3.17 (0.89)	1.90/2.40 (0.89)	1.21/2.73 (0.89)	1.34/2.67 (1.73)	3.93/4.48 (1.14)
ZnP$_2$-CMP	1130	1.75	0.8-2	2.09[b] (1.23)[c]	2.42 (1.29)	6.01 (1.34)	6.86 (1.34)	6.05 (1.33)	4.50 (2.61)	5.45 (1.72)
ZnP$_1$-LP	-	-	-	0.24[b]	0.65	0.60	0.70	0.75	0.75	0.80
YP-17	2100	1.07	1.2	0.76[b]	0.79	0.82	0.82	0.82	1.09	1.05

[a] Capacity for vapor. [b] Capacity for liquid. [c] Theoretical capacity calculated based on the pore volume and amine density.

Section 8. TGA Profiles of MP$_1$-CMPs upon Adsorption of Amines

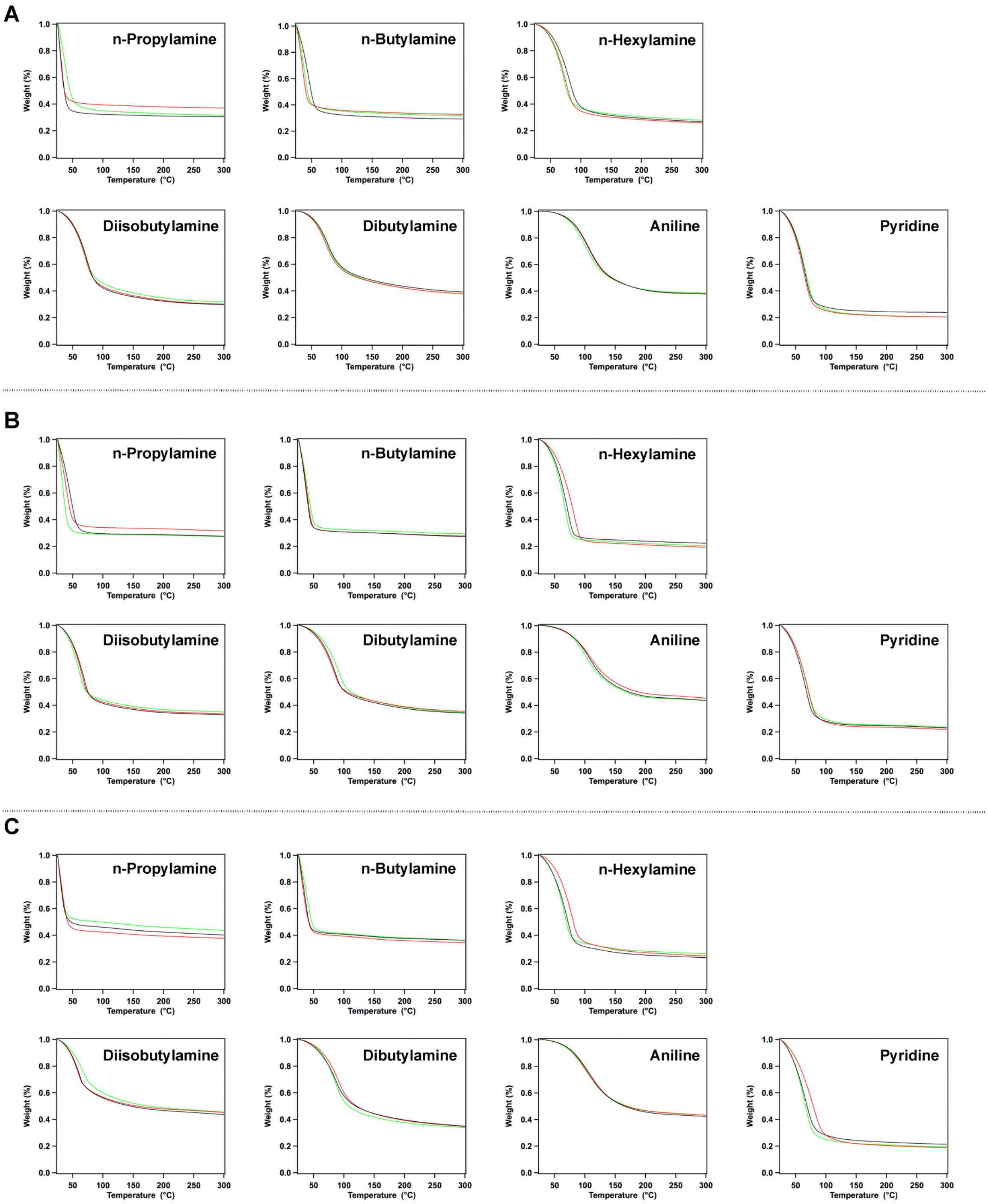

Figure S6. TGA profiles of A) ZnP$_1$-CMP, B) CuP$_1$-CMP, and C) CoP$_1$-CMP, upon uptake of amine vapors. Three experiments were performed for each amine.

Section 9. Porosity Effect on the Uptake of Amine

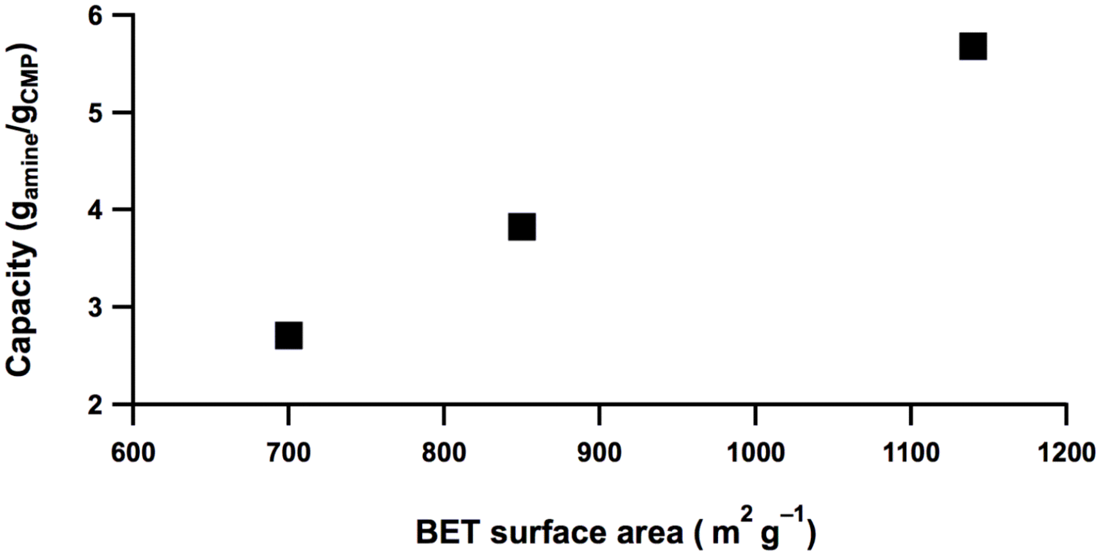

Figure S7. The uptake of pyridine liquid by the ZnP_1-CMP samples with different porosity.

Section 10. Porous Structure of Activated Carbon YP-17

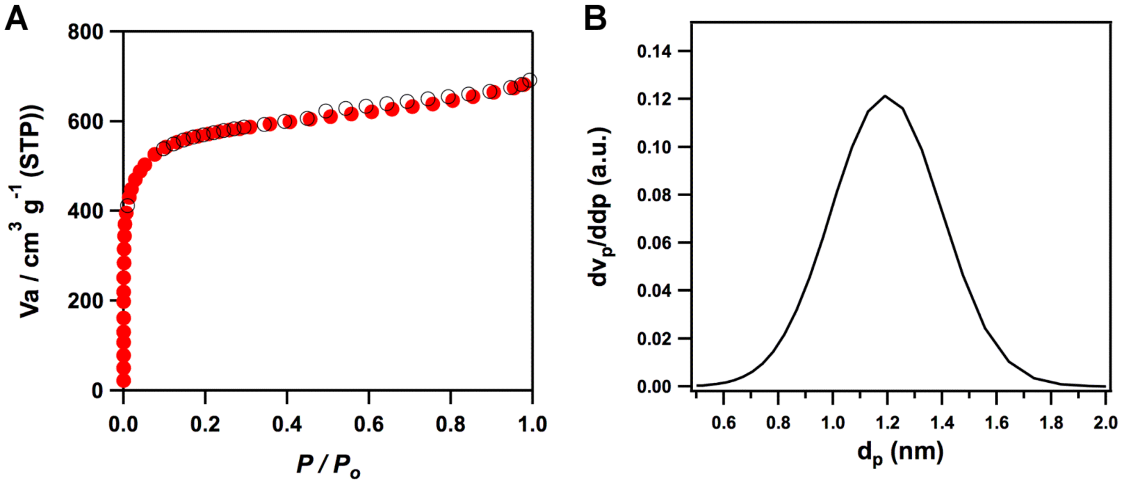

Figure S8. A) Nitrogen sorption isotherm profile of activated carbon YP-17. B) Pore size distribution of YP-17.

Section 11. Cycle Use

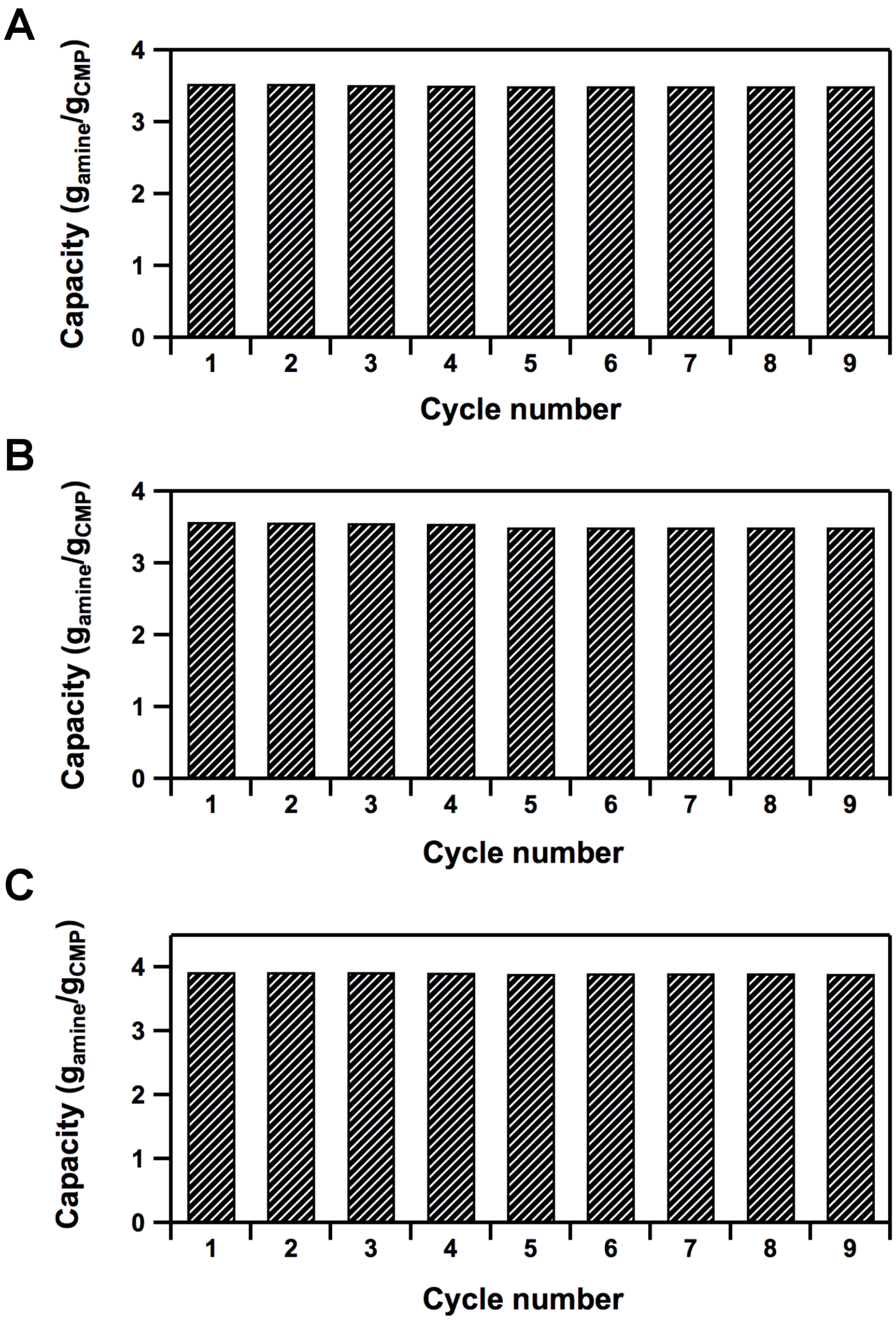

Figure S9. Cycle use of A) ZnP_1-CMP, B) CuP_1-CMP, and C) CoP_1-CMP for the uptake of pyridine vapor.